Quantum-Chemical (Density Functional Theory) Study of Lithium 2-Methoxyethoxide, Methyl α-Lithioisobutyrate, and Their Mixed Aggregates as Models of the Active Center in the Anionic Polymerization of Methacrylates

Alexander V. Yakimansky† and Axel H. E. Müller*

Institut für Physikalische Chemie, Johannes Gutenberg Universität, Welderweg 15, D-55099 Mainz, Germany

Received September 24, 1998; Revised Manuscript Received December 29, 1998

ABSTRACT: Density functional theory calculations of stabilities of various aggregates of lithium 2-methoxyethoxide (MEO−Li), methyl α-lithioisobutyrate (MIB−Li), and their mixtures show that hexameric structures of prismatic type are most stable. The calculated NMR shifts at the α-carbon atoms of these aggregates correctly reproduce the experimental dependence of the shifts on the molar ratio MEO−Li/MIB−Li. Since these mixtures are models for the active center in the anionic polymerization of methyl methacrylate (MMA), it is demonstrated that some of these mixed aggregates are able to coordinate an MMA molecule. The resulting complex is very stable and has a geometry suitable for the monomer addition reaction, i.e., the bond formation between the MIB−Li α-carbon and the monomer vinyl group.

Introduction

Lithiated ester enolates are intermediates in many organic reactions, but their most important application is as initiators of the anionic polymerization of (meth)-acrylates, especially methyl methacrylate (MMA).[1,2] In principle, they are ideally suited for this task since they are models of the active center of these polymerizations. Consequently, the structure of these compounds has been studied extensively. Seebach[3,4] showed that various ester enolates are aggregated in the crystalline state. Vapor pressure osmometry[5] show that lithiated isobutyrates are aggregated in solution, the average degree of aggregation being $n = 2-4$ in polar solvents, like THF, and 4 to >6 in nonpolar solvents, like toluene. These findings were confirmed by ^{13}C and ^{7}Li NMR studies of Wang and Teyssié,[6] who found a dynamic equilibrium between dimers and tetramers of methyl α-lithioisobutyrate (MIB−Li) in THF, the tetramer being more stable at higher temperatures. NMR measurements of Kříž et al.[7] even indicate the presence of trimers. NMR measurements of ethyl α-lithioisobutyrate (EiB−Li) in toluene[8] also indicate strong aggregation.

Recent ab initio (Hartree−Fock) and semiempirical studies of MIB−Li aggregates ($n = 1$, 2, and 4)[9] show that, with increasing degree of aggregation, the structures become more stable but less polar and the electron densities on the C_α atoms of the enolates decrease, leading to (calculated) downfield shifts which well correlate with the observed shifts. Specific and nonspecific solvation by THF leads to a quantitative but not to a qualitative change of this behavior.

Consequently, aggregation of ester enolates leads to a considerable decrease of their reactivity as initiators of anionic polymerization. In fact, in the anionic polymerization of MMA, initiated by MIB−Li in THF, it was shown that aggregates of the active chain end are some orders of magnitude less reactive than nonaggregated ion pairs.[10] In nonpolar solvents the polymerization proceeds in an uncontrolled manner, leading to very broad and multimodal molecular weight distributions.[11] This may be attributed to the coexistence of various aggregated species of different reactivity that exchange only slowly on the polymerization time scale.

It is, thus, important to decrease the aggregation or at least to suppress the formation of higher aggregated ester enolates which are of extremely low reactivity. For this aim, polar solvents, especially THF or 1,2-dimethoxyethane, and larger counterions have been used, resulting in a controlled polymerization.[12,13] In some more recent approaches, various ligands have been introduced as additives. σ-Ligands, i.e., electron donors, specifically solvate the Li atoms of the ester enolate individual molecules or aggregates, thus preventing their further aggregation. Such electron donors, like cryptands,[14,15] crown ethers,[16] glymes,[15] or diamines,[17] have been used, and their effects on the state of aggregation of lithiated ester enolates and polymerization kinetics have been studied experimentally. Alternatively, μ-ligands, especially alkali halides, have been used with much success.[18] It was shown that these ligands break up the aggregation of the ester enolate chain ends by forming mixed aggregates.[10]

Recently, lithium alkoxyalkoxides of the type $Li-(O-CH_2-CH_2)_m-OCH_3$ ($m = 1$, 2) have been shown to be extremely efficient additives for the anionic polymerization of MMA and acrylates even in nonpolar solvents, like toluene.[19] These compounds combine the properties of σ- and μ-ligands in one molecule. We found that the polymerization of MMA initiated by diphenylhexyllithium (DPH−Li) in the presence of lithium 2-methoxyethoxide (MEO−Li) at molar ratios $r = [MEO-Li]/[DPH-Li] \geq 5$ in toluene is extremely fast with half-lives of fractions of seconds at room temperature.[20] The rate constants are comparable to those observed in the presence of cryptands.[14] Moreover, the tacticity of the obtained polymers changes from isotactic to highly syndiotactic. These data suggest the deaggregation of

† Permanent address: Institute of Macromolecular Compounds of the Russian Academy of Sciences, Bolshoi prospect 31, 199004 St. Petersburg, Russia.

10.1021/ma981514+ CCC: $18.00
Published on Web 03/23/1999

the chain end and the formation of species of extremely high reactivity. In contrast, initiation by ethyl α-lithioisobutyrate (EiB−Li) leads to long induction periods and less controlled polymerization. The latter finding demonstrates that low molecular weight ester enolates are not perfect models of the active polymer chain end since they cannot model the electronic and steric effects of the neighboring polymer segments. It is assumed that the pending polymer chain will decrease the tendency to form aggregates, especially those of more than two chain ends.

One could not predict lithium alkoxyalkoxides to be so efficient in deaggregation of ester enolates, because alkoxides are well-known to be aggregated themselves.[21] Wang et al.[22] presented ^{13}C NMR studies of methyl α-lithioisobutyrate (MiB−Li) in the presence of lithium 2-(2-methoxyethoxy)ethoxide ($m = 2$, MEEO−Li)) in THF and THF/toluene mixtures. The α-carbon shows a strong upfield shift at ratios $r = [\text{MEEO−Li}]/[\text{MIB−Li}] \geq 2$. This was attributed to the formation of "ligand-separated" ion pairs where the lithium ion of the enolate is surrounded by two coordinating lithium alkoxyalkoxide molecules. Recent NMR studies on interactions of MEEO−Li with di-*tert*-butyl 2-lithio-2,4,4-trimethylglutarate in THF[36] and of MEO−Li with EiB−Li in toluene[23] also show an upfield shift of the α-carbon, but this shift is by far less pronounced than the one observed by Wang et al. It was concluded that various mixed aggregates of the ester enolate and the alkoxyalkoxide might form, depending on the stoichiometry of the two compounds.

The aim of the present paper is twofold: we first will calculate the most stable structures of MIB−Li, as a model of the toluene-soluble ester enolate EIB−Li and of the chain end of PMMA−Li, and of lithium 2-methoxyethoxide (MEO−Li), $LiOCH_2CH_2OCH_3$, and their mixed aggregates employing the density functional theory (DFT) approach.[24] It is beyond the scope of this paper to calculate transition states for the addition of monomer to these complexes. Also, we cannot exclude that small amounts of less stable species (in equilibrium with more stable ones) are the true active species in real polymerizing systems. However, we will try to estimate the ability of the calculated complexes to interact further with MMA in order to promote the polymerization.

Methods

All quantum-chemical calculations were carried out employing the TURBOMOLE package[25] of ab initio quantum chemical programs within the framework of the DFT approach.[24]

The geometries of all studied structures of the type $(\text{MIB−Li})_n(\text{MEO−Li})_x(\text{MMA})_y$ were completely optimized. For the DFT geometry optimizations, Becke's exchange potential[26] and Perdew's correlation potential[27] were used. We refer to this set of DFT potentials as BP86.

For the geometry optimizations we used the TURBOMOLE split valence plus polarization (SVP) basis sets[28] consisting of (1) (7s4p)/[3s2p] basis sets augmented with one d-polarization function for carbon (d-exponent 0.8) and oxygen (d-exponent 1.2), (2) (7s)/[3s] basis set for lithium augmented with one p-polarization function (p-exponent 0.17), and (3) double-ζ (4s)/[2s] basis set for hydrogen.

The TURBOMOLE modules for the geometry optimizations were RIDFT (for energy calculations) and RDGRAD (for energy gradient calculations), employing the RI approximation[29] for the Coulomb potential. The RI approximation makes use of the molecular electron density representation in terms of an atom-centered auxiliary basis set (ABS). This makes it possible to approximate the Coulomb potential with high accuracy, avoiding the calculations of four-centered two-electron integrals.[29] The ABS specially optimized for use with SVP basis sets were (8s3p3d1f)/[6s3p3d1f] basis sets for carbon and oxygen, (8s2p2d1f)/[6s2p2d1f] basis set for lithium, and (4s2p)/[2s1p] basis set for hydrogen.[29]

For all the geometries optimized at SVP-ABS/BP86 level, single-point energy calculations were performed with Becke's three-parameter functional,[30] including a mixture of Hartree−Fock exchange with DFT exchange correlation, and the correlation potential by Lee, Yang, and Parr,[31] including both local and nonlocal terms. We refer to this set of DFT potentials as B3LYP. For these single-point energy calculations, the Karlsruhe TZV basis sets[32] of triple-ζ quality were augmented with one p-polarization function for hydrogen (p-exponent 0.8) and with the same polarization functions for carbon, oxygen, and lithium as those included into SVP basis sets. The resulting basis set is hereafter referred to as TZVP.

To check the reliabilities of the structures found, ^{13}C NMR spectra were also calculated by the GIAO−SCF method[33] implemented into the TURBOMOLE program.[34] For the NMR calculations of all structures studied, Hartree−Fock molecular orbitals calculated at the TZVP level for the geometries optimized at the SVP-ABS/BP86 level were used. The changes in the calculated ^{13}C NMR shifts at C_α atoms of MIB−Li fragments with the increase of x/n ratio were compared to the experimental observations.[23]

For all considered structures of the type $(\text{MIB−Li})_n(\text{MEO−Li})_x(\text{MMA})_y$, the values of a single comparable stability parameter, the averaged energy per one MIB−Li molecule, $\bar{E}$, were calculated via eq 1:

$$n\bar{E} = E[(\text{MIB−Li})_n(\text{MEO−Li})_x(\text{MMA})_y] - x\bar{E}_{\min}(\text{MEO−Li}) - yE(\text{MMA}) \quad (1)$$

where $E[(\text{MIB−Li})_n(\text{MEO−Li})_x(\text{MMA})_y]$ is the minimized total energy of the particular complex $(\text{MIB−Li})_n(\text{MEO−Li})_x(\text{MMA})_y$ and $\bar{E}_{\min}(\text{MEO−Li})$ is the total minimized energy per one MEO−Li molecule of the most stable $(\text{MEO-Li})_x$ aggregate.

All calculations are for vacuum conditions; however, it is believed that the effect of the nonpolar toluene molecules will not significantly perturb the results obtained.

Results and Discussion

Structure of Pure Lithium 2-Methoxyethoxide (MEO−Li). It is well-known that lithium alkoxides are aggregated in nonpolar solvents with degrees of aggregation $n \geq 4$. For MEO−Li, the average degree of aggregation in hexamethylphosphoramide was found to be $\bar{n} = 5$ by cryoscopic measurements.[35] Therefore, tetrameric $(\text{MEO−Li})_4$ and hexameric $(\text{MEO−Li})_6$ aggregates were calculated. Their optimized geometries are displayed in Figure 1. The tetramer $(\text{MEO−Li})_4$ has S_4 symmetry and a "cubic" central core of Li−O bonds (Figure 1a), while the hexamer $(\text{MEO−Li})_6$ has S_6 symmetry and a prismatic central core (Figure 1b). In both aggregates, the terminal methoxy oxygens are

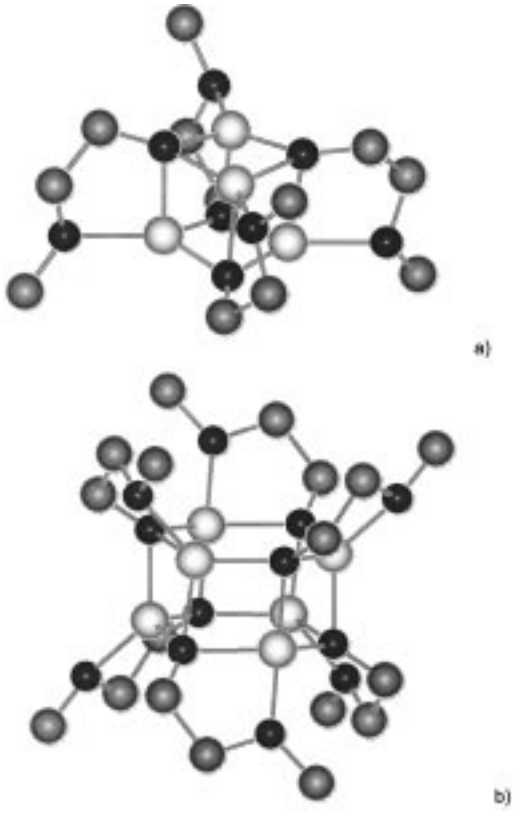

Figure 1. Optimized geometries of (a) $(MEO-Li)_4$ and (b) $(MEO-Li)_6$.

bound to Li atoms of the central core by a kind of "side-chain" coordination. Their total energies, E, and energies per one molecule, $\bar{E}$, are presented in Table 1. They show that the hexamer is more stable than the tetramer by ca. 10 kJ/mol per MEO−Li molecule. At both SVP-ABS/BP86 and TZVP/B3LYP levels, very close estimations of their relative stabilities were obtained. In terms of free energy this difference may be somewhat decreased but presumably not reverted due to an entropy loss at higher degrees of aggregation. Therefore, the $\bar{E}$ value for the hexamer was taken as $\bar{E}_{min}$(MEO−Li) to estimate via eq 1 the relative stabilities of the complexes containing MIB−Li molecules.

Another possible S_4 structure of the tetramer $(MEO-Li)_4$, consisting of an eight-membered ring of alternating Li and O atoms in the central core, was found to be much less stable than the S_4 structure with the "cubic" central core. Therefore, only the latter one is presented and discussed here. However, for lithium 2-(2-methoxyethoxy)ethoxide (MEEO−Li), a tetrameric structure with the eight-membered ring central core was recently reported as the most stable on the basis of 3-21G ab initio calculations.[36] It is difficult to assign this discrepancy between the MEO−Li and MEEO−Li most stable tetrameric structures to the structural differences between the MEEO−Li and MEO−Li molecules because in the eight-membered ring of the $(MEEO-Li)_4$ tetramer presented in ref 36, the terminal methoxy oxygens do not at all participate in the Li−O coordination. Therefore, we believe that the "cubic" structure of tetrameric lithium alkoxyalkoxide aggregates, being the most stable one at a much higher level of theory than that used in ref 36, is more reasonable than the alternative eight-membered cyclic structure.

It is of particular interest to discuss the ^{13}C NMR shifts at the C-atoms of the MEO−Li molecule

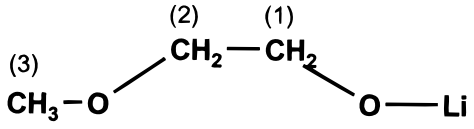

MEO-Li

within the tetrameric and hexameric MEO−Li aggregates. The calculated ^{13}C NMR shifts for these aggregates are shown in Table 2 and compared to the experimental ones.[23] It is seen that the state of MEO−Li aggregation does not cause a considerable effect on the calculated ^{13}C NMR shifts. The reason is probably that the polarities of Li−O bonds, primarily determining the ^{13}C NMR shifts, are similar in the two aggregates, as lithium atoms in both of them are in a more or less tetrahedral surrounding by the four oxygen atoms. From the fact that more than one resonance per carbon atom is observed, it may be concluded that various species of comparable stability are present in toluene solution. These may differ in their aggregation number of the structure of a given aggregate. A systematic difference of ca. 4 ppm between the calculated and experimental values should be noted. However, the relative ^{13}C NMR shifts agree with the assignment of the most downfield signal (80.0 ppm) to the $^{(2)}C$ atom, made on the basis of $^{13}C/^{1}H$ COSY and $^{7}Li/^{1}H$ HOESY experiments,[23,36] and contradict the former assignment of this signal to the $^{(1)}C$ atom by Wang et al.[22]

Structure of Pure Methyl α-Lithioisobutyrate. In agreement with the experimental data, recent ab initio Hartree−Fock calculations[9] have shown that in the absence of the specific solvation of Li atoms (in a vacuum or nonpolar solvent, like toluene) a "cubic" S_4 tetramer $(MIB-Li)_4$ is considerably more stable than the planar dimer $(MIB-Li)_2$. In the present paper, DFT geometry optimization was performed for both the "cubic" S_4 tetramer $(MIB-Li)_4$ (Figure 2a) and the prismatic S_6 hexamer $(MIB-Li)_6$ (Figure 2b). As seen from Figure 2a,b, the S_4 tetramer consists of the two dimeric $(MIB-Li)_2$ fragments and the S_6 hexamer of two trimeric $(MIB-Li)_3$ fragments placed one above the other with the mutual rotation angle of 90° and 60°, respectively. It should be noted that in both aggregates there is a "side-chain" Li−O coordination of the alcohol oxygen atoms with Li atoms in the central cores (Figure 2a,b). Such a coordination brings about a considerable stabilization. In particular, the S_4 tetramer presented in Figure 2a is by ca. 16 kJ/mol per MIB−Li molecule more stable than the earlier reported[9] "cubic" tetramer of the same symmetry without "side-chain" Li−O coordination. However, even the S_4 tetramer presented here is of considerably lower stability (by more than 13 kJ/mol) compared to the S_6 hexamer (Table 1). It is noteworthy that the $\Delta\bar{E}$ values of the S_4 tetramer obtained at SVP-ABS/BP86 and TZVP/B3LYP levels almost coincide.

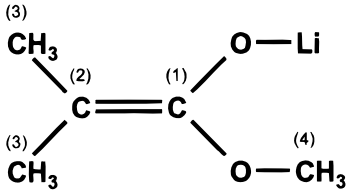

MIB-Li

Table 1. Calculated DFT Energies for Mixed $(MIB-Li)_n(MEO-Li)_xMMA_y$ Aggregates and the Pure Components

		E, hartrees		$\bar{E}$, hartrees		$\Delta\bar{E}$, kJ/mol	
	Fig	SVP-ABS/BP86	TZVP/B3LYP[a]	SVP-ABS/BP86	TZVP/B3LYP[a]	SVP-ABS/BP86	TZVP/B3LYP[a]
MMA		−345.532 975	−345.7121 34				
$(MEO-Li)_4$	1a	−1105.494 689	−1106.112 292	−276.373 672	−276.528 073	10.7	9.0
$(MEO-Li)_6$	1b	−1658.266 408	−1659.189 017	−276.377 735	−276.531 503	0	0
$(MIB-Li)_4$	2a	−1414.943 231	−1415.673 969	−353.735 808	−353.918 492	14.3	13.3
$(MIB-Li)_4$[b]		−1414.918 858	−1415.648 438	−353.729 715	−353.912 110	30.3	30.1
$(MIB-Li)_6$	2b	−2122.447 428	−2123.541 494	−353.741 238	−353.923 582	0	0
$(MIB-Li)_2(MEO-Li)_4$	3	−1812.998 715	−1813.978 646	−353.743 888	−353.926 317	−6.9	−7.2
$(MIB-Li)_1(MEO-Li)_5$	4a	−1735.632 894	−1736.584 249	−353.744 219	−353.926 735	−7.8	−8.3
$(MIB-Li)_1(MEO-Li)_5$	4b	−1735.630 323	−1736.581 059	−353.741 648	−353.923 545	−1.1	0.1
$(MIB-Li)_1(MEO-Li)_5$-MMA	5	−2081.173 701	−2082.296 915	−353.752 053	−353.927 267	−28.4	−9.7

[a] All geometries were optimized at the SVP-ABS/BP86 level. [b] Reference 9, Figure 5.

Table 2. Calculated and Measured ^{13}C NMR Shifts, δ, for Mixed $(MIB-Li)_n(MEO-Li)_xMMA_y$ Aggregates and the Pure Components; All Measurements[23] Performed in Toluene-d_5

		$^{(1)}C$	$^{(2)}C$		$^{(3)}C$
	Fig	δ, ppm	δ, ppm	$\Delta\delta$, ppm	δ, ppm
$(MEO-Li)_4$	1a	58.9	75.1		53.9
$(MEO-Li)_6$	1b	58.7	75.3		53.4
exp (25 °C)		62.8; 63.1	79.1; 79.4		57.7; 57.8
$(MIB-Li)_4$	2a	166.7	83.4		15.7; 15.8
$(MIB-Li)_6$	2b	166.1	85.4	0[a]	15.5; 15.7
exp (EIB−Li, 25 °C)		158.4−159.2	76.8−77.5	0[b]	17.0−18.3
$(MIB-Li)_2(MEO-Li)_4$ (Figure 3)	3	167.7	80.8	−4.6[a]	15.6; 16.2
exp (−20 °C, [MEO−Li]/[EIB−Li] = 2)		158.1−159.0	72.4−75.9	−4.4 to −1.6[b]	17.9−18.9
$(MIB-Li)_1(MEO-Li)_5$	4a	167.9	80.2	−5.2[a]	15.6; 16.3
$(MIB-Li)_1(MEO-Li)_5$	4b	169.7	79.5	−5.9[a]	15.7; 16.5
exp (−20 °C, [MEO−Li]/[EIB−Li] = 5)		158.6−159.3	70.9−72.9	−5.9 to −4.6[b]	18.1−19.2
$(MIB-Li)_1(MEO-Li)_5$MMA	5	169.2	79.0	−6.4	15.9; 17.07

[a] Differences between the calculated shifts at C_α carbons for the mixed $(MIB-Li)_n(MEO-Li)_x$ aggregates and the pure $(MIB-Li)_6$ aggregate. [b] Differences between the measured shifts at C_α carbons for the EIB−Li/MEO−Li mixtures and pure EIB−Li.

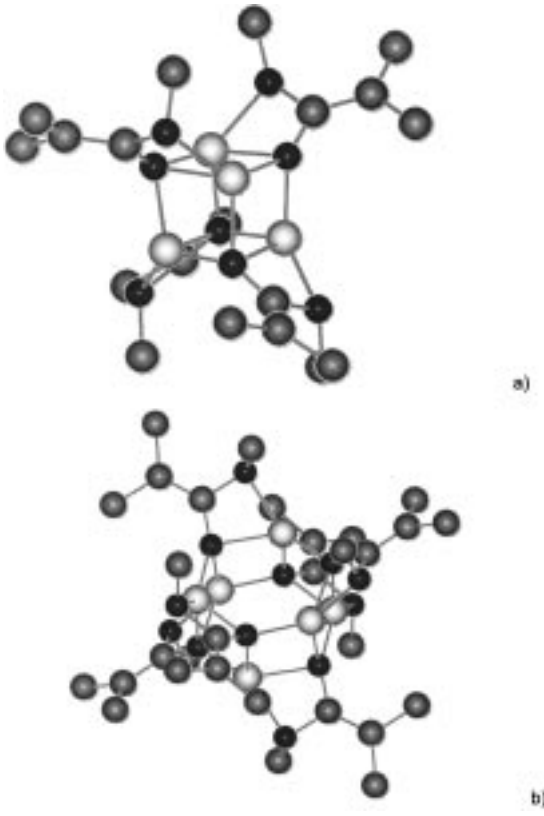

Figure 2. Optimized geometries of (a) $(MIB-Li)_4$ and (b) $(MIB-Li)_6$.

The calculated ^{13}C NMR shifts for the MIB−Li tetramer and hexamer and the measured ones for EIB−Li at room temperature in toluene-d_8 are presented in Table 2. Again, more than one resonance per carbon atom indicates multiple species in toluene solution. As seen from Table 2, for both MIB−Li aggregates, the calculated shifts of the methyl ($^{(3)}C$) carbons agree reasonably with the experimental data. Also, for both structures, calculated shifts at the carbonyl carbon ($^{(1)}C$) are shifted about 8−9 ppm downfield compared to the measured value. As to the calculated shifts at the α-carbon ($^{(2)}C$), for the hexamer it is shifted downfield by approximately the same amount compared to the measured value, while for the tetramer this downfield shift is about 6−7 ppm. Thus, the differences between the calculated and measured shifts at the $^{(1)}C$ and $^{(2)}C$ atoms (forming the double bond) look like a systematic underestimation of the calculated values by 6−9 ppm compared to observed ones. These deviations are well within the reported limits of 7−10 ppm[37] and may be due to unavoidable approximations behind the theoretical approach and to some experimental factors beyond the consideration within this approach (e.g., small but nonnegligible nonspecific solvation effect of toluene as dielectric continuum).

Mixed $(MIB-Li)_n(MEO-Li)_x$ Aggregates. Taking into account that, for both pure MEO−Li and pure MIB−Li, hexamers of prismatic architecture are most stable, the same prismatic type of hexameric complexes should be expected for mixed $(MIB-Li)_n(MEO-Li)_x$ aggregates, i.e., $x = 6 - n$. The maximum x/n ratio for such mixed aggregates is, obviously, 5 (for $n = 1$). As discussed in the Introduction, it was found experimentally that the rate of MMA polymerization increases with the molar ratio r = [MEO−Li]/[initiator] up to $r = 5$; a further increase has no effect on the polymerization rate constant. This experimental observation indicates that a hexameric mixed 1:5 aggregate $(MIB-Li)_1(MEO-Li)_5$ might be more reactive than other complexes of the structure $(MIB-Li)_x(MEO-Li)_{6-x}$. Thus, DFT geometry optimizations were performed for the 2:4 ($n = 2$, C_i symmetry, Figure 3) and 1:5 mixed complexes ($n = 1$, Figure 4a,b).

As seen from Figures 3 and 4, the structures of all mixed aggregates are of prismatic type. Their central prismatic cores consist of two almost planar six-membered cycles formed by Li−O bonds and placed one

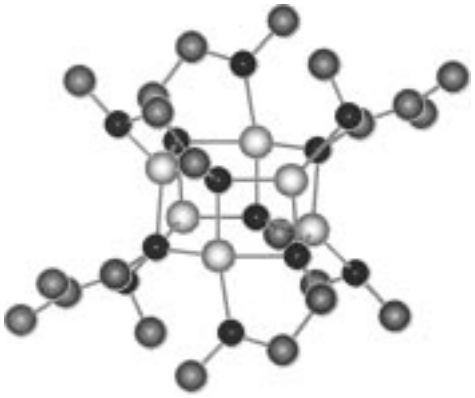

Figure 3. Optimized geometry of $(MIB-Li)_2(MEO-Li)_4$.

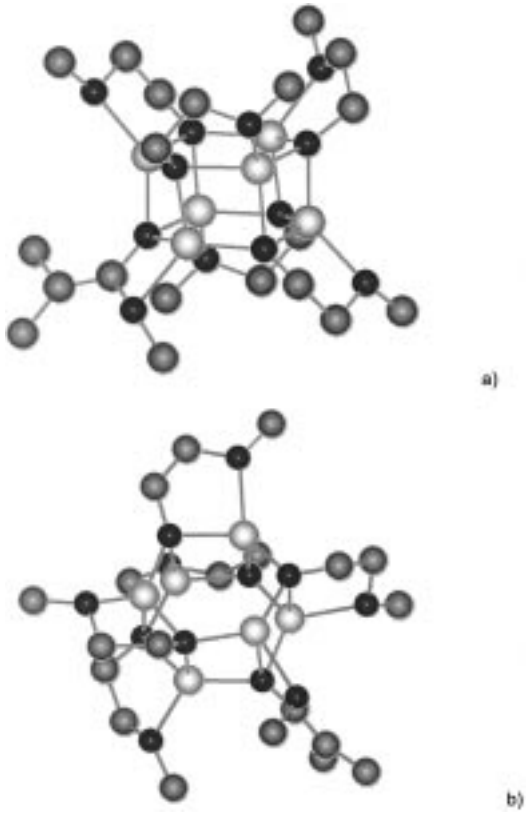

Figure 4. Optimized geometries of $(MIB-Li)_1(MEO-Li)_5$.

above the other. The optimized Li−O bond lengths within the cycles are in the range from 1.9 to 2.0 Å. One of these cycles is rotated with respect to the other by ca. 60° to provide six Li−O bond contacts (corresponding optimized bond lengths are about 2.0 Å) between the cycles. Each Li atom is, thus, bound to two oxygens within one of six-membered cycles and one oxygen in the other, the fourth "side-chain" Li−O bond (typical optimized bond lengths are about 2.06 Å) being formed with one of methoxy oxygens of either the MEO−Li or the MIB−Li fragment.

The two 1:5 complexes differ by the arrangement of "side-chain" Li−O contacts. In particular, for the 1:5 complex presented in Figure 4a, in contrast to that shown in Figure 4b, there are no "side-chain" Li−O bonds between the two six-membered cycles in the central prismatic core. Due to these structural differences, the former is more stable (i.e., has a more negative $\bar{E}$ value) than the latter (Table 1).

As the data in Table 1 show, the 2:4 complex (Figure 3) and one of 1:5 mixed complexes (Figure 4a) are more stable than pure MIB−Li aggregates, the 1:5 mixed complex shown in Figure 4a being the most stable one. It means that the formation of these complexes from pure MIB−Li and MEO−Li is exothermic and, thus, favorable. Since the total degree of aggregation does not change, only small entropy effects are expected.

Figure 5. Optimized geometry of $(MIB-Li)_1(MEO-Li)_5MMA$.

The calculated NMR shifts for the MIB−Li fragments of these mixed complexes are presented in Table 2 together with the experimental data measured in toluene-d_8 at −20 °C for $r = 2$ (2:4 aggregate) and $r = 5$ (1:5 aggregate). As seen from this table, NMR calculations exactly reproduce the experimental observation that there are no considerable changes of NMR shifts of the $^{(1)}$C and $^{(3)}$C atoms upon mixing MIB−Li and MEO−Li, while the NMR signal of the α-carbon ($^{(2)}$C) is shifted upfield up to ca. 5 ppm for $r = 5$. Since an upfield shift correlated with an increased charge density, this might partially explain the increased reactivity. However, it is hard to believe that the charge density increase brought about by the formation of the 1:5 complex is the only reason for the dramatic increase in reactivity by 3−4 orders of magnitude.

On the basis of their NMR spectra, Wang et al.[22] postulated the formation of "ligand-separated" ion pairs. SVP-ABS/BP86 calculations on the "ligand-separated" ion pair $MIB^-,Li^+(MEO-Li)_4$ resulted in an unreasonably high formation energy of >220 kJ/mol, indicating that such a charge-separated structure is highly improbable in nonpolar solvents. Thus, we wish to propose another possibility in order to explain the extreme increase in reactivity.

An important question is, to what extent are the mixed aggregates able to coordinate a monomer (MMA) molecule to promote the polymerization? The interaction of the monomer with one of Li atoms of mixed aggregates may change the surrounding of this and other Li atoms within these aggregates and even stabilize the structures that are not most favorable in the absence of the monomer. In particular, it was found that, as a result of the interaction of MMA with the 1:5 complex shown in Figure 4b, the "side-chain" Li−O bond between one of Li atoms and alcohol oxygen of the MIB−Li fragment was broken and replaced with the bond between the Li atom and MMA carbonyl oxygen. The DFT optimized geometry of the resulting $(MIB-Li)_1(MEO-Li)_5MMA$ complex is shown in Figure 5. As seen from Table 1, it is much more stable in comparison to all other complexes. The calculated NMR shift of its α-carbon of the MIB−Li fragment is lower compared to those of $(MIB-Li)_1(MEO-Li)_5$ complexes by 0.5−1.2 ppm (Table 2). It means that the electron density at the α-carbon and, hence, its reactivity somewhat increase due to the coordination to the monomer molecule. This

could, in fact, be expected because of the released "side-chain" coordination of alcohol oxygen of the MIB−Li fragment to one of Li atoms.

It is also important to stress that the α-carbon of the MIB−Li fragment in this $(MIB-Li)_1(MEO-Li)_5MMA$ complex is at the distance of only ca. 3.3 Å from the *β*-carbon of the MMA fragment which should make the direct interaction between them, i.e., monomer addition, rather favorable.

It should be noted that the $\Delta\bar{E}$ values calculated at SVP-ABS/BP86 and TZVP/B3LYP levels are very close for all 2:4 and 1:5 complexes discussed above, except for the $(MIB-Li)_1(MEO-Li)_5MMA$ complex. The latter is still the most stable one at both levels. However, its stability at the TZVP/B3LYP level does not exceed those of other complexes so considerably as at the SVP-ABS/BP86 level.

Conclusions

The presented DFT and NMR calculation results clearly indicate that the most stable complexes formed in the mixtures of MIB−Li and MEO−Li in nonpolar solvents are of hexameric prismatic type (Figures 3−5), the formation of mixed $(MIB-Li)_n(MEO-Li)_{6-n}$ aggregates from the pure components being exothermic. Experimentally observed relative changes in the ^{13}C NMR shifts of the α-carbon with increasing molar ratio of alkoxyalkoxide to initiator are well reproduced by the calculated NMR shifts. It is shown that the reactivity of these mixed aggregates may increase due to the interaction with MMA monomer molecule. However, we cannot exclude that small amounts of less stable species (in equilibrium with the more stable ones) are the true active species in real polymerizing systems.

Our data show that the mixed aggregate structures $(MIB-Li)_n(MEO-Li)_{6-n}$ discussed above are reasonable intermediates in MMA polymerization processes in the presence of lithium alkoxyalkoxides. Although MIB−Li is not a perfect model of the living chain end, the calculated complexes represent the most probable structures of living PMMA−Li in the presence of MEO−Li in nonpolar solvents. MNDO calculations of mixed aggregates of MEEO−Li with di-*tert*-butyl 2-lithio-2,4,4-trimethylglutarate[36] have led to a number of different types of living chain end architectures. However, these structures seem to be doubtful because they are not thermodynamically stable.[36] Moreover, some of these MNDO structures include $Li-C_\alpha$ coordination bonds which, in the aggregates of this type, are usually a consequence of the well-known artifact of the MNDO method.[9,38−40]

Acknowledgment. This work was supported by INTAS (Grant INTAS-RFBR 95-165). A.Y. expresses his gratitude to the Deutsche Forschungsgemeinschaft for financial support.

Supporting Information Available: Cartesian coordinates (in atomic units) of the structures in Figures 1−5. This material is available free of charge via the Internet at http://pubs.acs.org.

References and Notes

(1) Lochmann, L.; Rodová, M.; Petránek, J.; Lím, D. *J. Polym. Sci., Polym. Chem. Ed.* **1974**, *12*, 2295.
(2) Lochmann, L.; Rodová, M.; Trekoval, J. *J. Polym. Sci., Polym. Chem. Ed.* **1974**, *12*, 2091.
(3) Seebach, D.; Amstutz, R.; Laube, T.; Schweizer, W. B.; Dunitz, J. D. *J. Am. Chem. Soc.* **1985**, *107*, 5403.
(4) Seebach, D. *Angew. Chem.* **1988**, *100*, 1685.
(5) Halaska, V.; Lochmann, L. *Collect. Czech. Chem. Commun.* **1973**, *38*, 1780.
(6) Wang, J. S.; Jérôme, R.; Warin, R.; Teyssié, P. *Macromolecules* **1993**, *26*, 1402.
(7) Kříž, J.; Dybal, J.; Vlcek, J. *Macromol. Chem. Phys.* **1994**, *195*, 3039.
(8) Schlaad, H.; Kolshorn, H.; Müller, A. H. E. *Macromol. Rapid Commun.* **1994**, *15*, 517.
(9) Weiss, H.; Yakimansky, A. V.; Müller, A. H. E. *J. Am. Chem. Soc.* **1996**, *118*, 8897.
(10) Kunkel, D.; Müller, A. H. E.; Lochmann, L.; Janata, M. *Makromol. Chem., Macromol. Symp.* **1992**, *60*, 315.
(11) Wiles, D. M.; Bywater, S. *Trans. Faraday Soc.* **1965**, *61*, 150.
(12) Kraft, R.; Müller, A. H. E.; Höcker, H.; Schulz, G. V. *Makromol. Chem., Rapid Commun.* **1980**, *1*, 363.
(13) Kraft, R.; Müller, A. H. E.; Höcker, H.; Schulz, G. V. *Makromol. Chem., Rapid Commun.* **1980**, *1*, 363.
(14) Johann, C.; Müller, A. H. E. *Makromol. Chem., Rapid Commun.* **1981**, *2*, 687.
(15) Wang, J. S.; Jérôme, R.; Warin, R.; Zhang, H.; Teyssié, P. *Macromolecules* **1994**, *27*, 3376.
(16) Wang, J. S.; Jérôme, R.; Teyssié, P. *Macromolecules* **1994**, *27*, 4615.
(17) Marchal, J.; Gnanou, Y.; Fontanille, M. *Makromol. Chem., Macromol. Symp.* **1996**, *107*, 27.
(18) Fayt, R.; Forte, R.; Jacobs, R.; Jérôme, R.; Ouhadi, T.; Teyssié, P.; Varshney, S. K. *Macromolecules* **1987**, *20*, 1442.
(19) Wang, J.-S.; Jérôme, R.; Bayard, P.; Patin, M.; Teyssié, P. *Macromolecules* **1994**, *27*, 4635.
(20) Maurer, A. R.; Marcarian, X.; Müller, A. H. E.; Navarro, C.; Vuillemin, B. *Polym. Prepr. (Am. Chem. Soc., Div. Polym. Chem.)* **1997**, *38* (1), 467.
(21) Halaska, V.; Lochmann, L.; Lím, D. *Collect. Czech. Chem. Commun.* **1968**, *33*, 3245.
(22) Wang, J.-S.; Jérôme, R.; Teyssié, P. *Macromolecules* **1994**, *27*, 4896.
(23) Maurer, A. R. Dissertation, Universität Mainz, 1998. Maurer, A. R.; Müller, A. H. E.; Kolshorn, H.; Mathiasch, B.; Bauer, W., manuscript in preparation.
(24) Parr, R. G.; Yang, W. *Density-Functional Theory of Atoms and Molecules*; Oxford University Press: Oxford, 1989.
(25) Ahlrichs, R.; Bär, M.; Häser, M.; Horn, H.; Kölmel, C. *Chem. Phys. Lett.* **1989**, *162*, 165.
(26) Becke, A. D. *Phys. Rev. A.* **1988**, *38*, 3098.
(27) Perdew, J. P. *Phys. Rev. B* **1986**, *33*, 8822.
(28) Schäfer, A.; Horn, H.; Ahlrichs, R. *J. Chem. Phys.* **1992**, *97*, 2571.
(29) Eichkorn, K.; Treuter, O.; Öhm, H.; Häser, M.; Ahlrichs, R. *Chem. Phys. Lett.* **1995**, *242*, 652.
(30) Becke, A. D. *J. Chem. Phys.* **1993**, *98*, 5648.
(31) Lee, C.; Yang, W.; Parr, R. G. *Phys. Rev. B.* **1988**, *37*, 785.
(32) Schäfer, A.; Huber, C.; Ahlrichs, R. *J. Chem. Phys.* **1994**, *100*, 5829.
(33) Ditchfield, R. *Mol. Phys.* **1974**, *27*, 789.
(34) Häser, M.; Ahlrichs, R.; Baron, H. P.; Weis, P.; Horn, H. *Theor. Chim. Acta* **1992**, *83*, 455.
(35) Tomoi, M.; Sekiya, K.; Kakiuchi, H. *Polym. J.* **1974**, *6*, 438.
(36) Zune, C.; Dubois, P.; Jérôme, R.; Kříž, J.; Dybal, J.; Lochmann, L.; Janata, M.; Vlcek, J.; Werkhoven, T. M.; Lugtenburg, J. *Macromolecules* **1998**, *31*, 2731.
(37) Gauss, J. *J. Chem. Phys.* **1993**, *99*, 3629.
(38) Dybal, J.; Kříž, J. *Collect. Czech. Chem. Commun.* **1994**, *59*, 1699.
(39) Dybal, J.; Kříž, J. *Collect. Czech. Chem. Commun.* **1995**, *60*, 1609.
(40) Dybal, J.; Kříž, J. *Macromol. Theory Simul.* **1997**, *6*, 437.

MA981514+